

Lifelong Topological Visual Navigation

Rey Reza Wiyatno¹, Anqi Xu², and Liam Paull¹

Abstract—The ability for a robot to navigate with only the use of vision is appealing due to its simplicity. Traditional vision-based navigation approaches required a prior map-building step that was arduous and prone to failure, or could only exactly follow previously executed trajectories. Newer learning-based visual navigation techniques reduce the reliance on a map and instead directly learn policies from image inputs for navigation. There are currently two prevalent paradigms: end-to-end approaches forego the explicit map representation entirely, and topological approaches which still preserve some loose connectivity of the space. However, while end-to-end methods tend to struggle in long-distance navigation tasks, topological map-based solutions are prone to failure due to spurious edges in the graph. In this work, we propose a learning-based topological visual navigation method with graph update strategies that improve lifelong navigation performance over time. We take inspiration from sampling-based planning algorithms to build image-based topological graphs, resulting in sparser graphs yet with higher navigation performance compared to baseline methods. Also, unlike controllers that learn from fixed training environments, we show that our model can be finetuned using a relatively small dataset from the real-world environment where the robot is deployed. We further assess performance of our system in real-world deployments.¹

I. INTRODUCTION

One key challenge for general-purpose autonomous mobile robots is the arduous setup requirements for operating in a new environment. Traditionally, a robot must first be piloted to build a metric map using methods like Simultaneous Localization and Mapping (SLAM) [1], which often requires costly equipment. An alternative appealing strategy is to forego the metric map and maintain a *topological* representation of the environment [2]. In such a setup, each edge in the graph encodes the traversability between two locations, while a local controller is used to actually navigate the edge.

Another limitation of metric-based navigation is that specifying goals in metric space is not intuitive. Ideally, navigation goals should carry semantic meaning, such as images of target objects or locations. While we see the emergence of learning-based methods that directly map images to actions [3], these policies tend to be reactive, are not data efficient, and are not suitable for long-distance navigation.

Our method builds a graph where each node corresponds to a particular image of a location. Fig. 1 illustrates how our agent uses the graph for planning a navigation task in

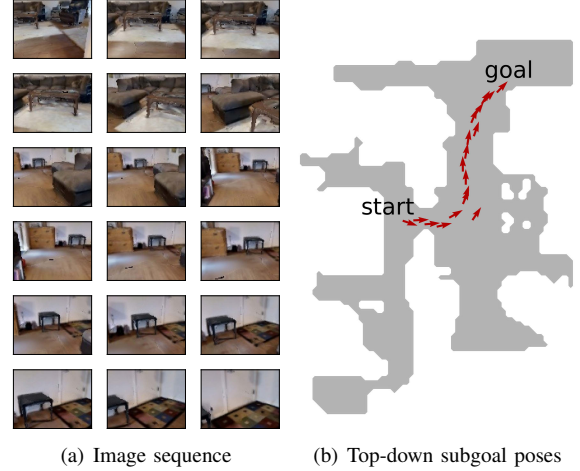


Fig. 1. A sample plan produced with our method to move from the top-left to the bottom-right image. The intermediary subgoal images transition smoothly, which helps the image-based controller easily navigate to the goal.

the image space. A crucial component of the system is a trained model for estimating connectivity and traversability between nodes. False positives from this model will cause the robot to try to execute potentially infeasible plans, while false negative predictions may result in failure to find a feasible plan when one actually exists. Compared with other learning-based topological navigation methods [4], [5], [6], we share a common algorithmic structure, as shown in Fig. 2, yet differ in choices for the learned model, data collection procedure, graph building approach, what graph edges encode, controller used, and graph update strategy.

To help with graph building, localization, and control, we train our single neural model to take two images and jointly predicts if one is reachable from the other, and, if so, their relative transformation in $SE(2)$. While we initially train this model using simulated maps, we can later finetune it in the target (e.g., real-world) environment by collecting a small added set of trajectory images. We take inspiration from sampling-based motion planners such as Probabilistic Roadmaps (PRM) [7] and Rapidly-exploring Random Tree (RRT) [8] to build a topological graph, by sampling nodes from a pool of collected images and using our model to determine their connectivity. During navigation, our agent continuously refines the graph based on its experience, to improve lifelong navigation performance.

The main contributions of our method are as follows:

- 1) We develop a sampling-based graph building process that produces sparser graphs and improves navigation performance,

¹Rey Reza Wiyatno and Liam Paull are with Montréal Robotics and Embodied AI Lab (REAL) and DIRO at the University of Montréal, QC H3T 1J4, Canada, and Mila, QC H2S 3H1, Canada rey.wiyatno@umontreal.ca, paull@iro.umontreal.ca

²Anqi Xu conducted this work with support from his past affiliation with Element AI, H2S 3G9, Canada anqi.xu@mail.mcgill.ca

¹Project page: <https://montrealrobotics.ca/ltvn/>

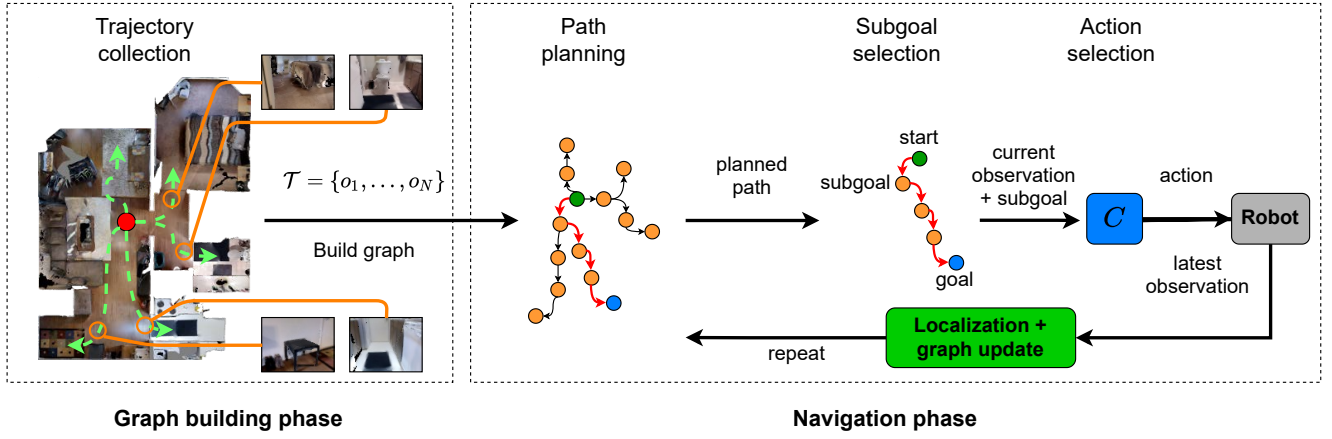


Fig. 2. Our navigation framework consists of separate graph building and navigation phases. During graph building, the robot first collects observations from the environment and builds a topological graph using a previously learned model. Later, during navigation, the agent is given a query (i.e., a goal observation), localizes itself on the graph, and plans a path to it. The agent picks a subgoal from the path, predicts what action to take to reach the subgoal, then executes it using a controller. The agent then relocalizes itself and updates the graph using its latest observation.

- 2) Our model can be finetuned in a target domain using only a small amount of data while yielding large performance gains,
- 3) We propose a graph update procedure that enables the graph to be continually refined during operation, which further improves lifelong navigation performance as the agent executes more queries.

Our evaluations show that our method outperforms the baselines when deployed in various simulated environments. We also show how our graph updates significantly improves navigation performance over time. Finally, we demonstrate strong system performance in the real world.

II. RELATED WORKS

Learning-based approaches have shown promising results in solving visual navigation tasks. For example, Zhu *et al.* [3] trained an end-to-end reinforcement learning (RL) policy that navigates based on a goal image. Training RL policies requires significant computation and time however, and thus is impractical to do in real-world environments. These end-to-end methods also typically do not work well in long-distance navigation tasks. In this work, we achieve lifelong navigation by combining a learning-based approach with topological graph-building and continuous refinements.

More closely related to our approach is Semi-parametric Topological Memory (SPTM) [4], which builds a graph using a trained classifier that predicts if two images are close, as measured by temporal distance during trajectory collection. However, as the graph edges are unweighted, false positive edges may be repeatedly chosen during planning, thus hampering navigation efficacy.

Similar to SPTM, Visual Navigation with Goals (ViNG) [6] regresses the number of steps required to move from one image to another, and uses this to weigh each edge. As a common concern with SPTM and ViNG, they build a navigation graph using *all* images within the collected trajectories, which poses scalability issues. Also, these methods

build the graph without considering the capability of their controller, which may result in edges that are not traversable in practice. Moreover, by solely relying on temporal distance within collected trajectories, these methods are blind to image pairs that are spatially close, yet temporally far within the explored trajectories circumstantially.

Bayesian Relational Memory (BRM) [9] builds a fully-connected graph where nodes and edges map to room types and the probability of room connectivity. BRM trains a classifier that predicts the probability of an image belonging to different room types. As the agent navigates, edge weights are refined using Bayesian updates. Our graph update strategy is similar to BRM, yet we also introduce new nodes to the graph to improve lifelong navigation performance.

Meng *et al.* [5] proposed a controller-dependent graph building method. At its core, a classifier is trained based on the controller rollout outcome in simulation to predict if an image pair is reachable. To build the graph, this classifier model is used to first sparsify highly reachable redundant nodes in the trajectories. Then, remaining nodes are connected with edges weighted by predicted reachability scores. As a drawback, it is impractical to finetune this reachability model in the real world, as it would require empirically unsafe controller rollouts between location pairs.

Other methods rely on an actor-critic model to evaluate graph connectivity using the critic [10], [11], [12]. Scott *et al.* [12] further sparsified the graph by only adding perceptually distinct nodes, merging nodes with shared connections, limiting the number of edges per node, and removing edges predicted as not traversable during test time. However, these sparsification strategies may lead to excessive false negative edges and poor connectivity. Also, such simulation-trained policies may not transfer well to real-world environments.

III. PROPOSED METHOD

Our work focuses on visual navigation tasks with images as goals. When we deploy our agent in a target environment,

we first execute a trajectory collection phase to obtain a pool of RGBD images $\mathcal{T} = \{o_1, \dots, o_N\}$, $o_i \in \mathcal{I}$. We then use \mathcal{T} to build a graph $G = (V, E)$, where vertices V are a subset of the collected images, and directed edges E are weighted by geodesic distance from one node to another.

During navigation, we present the agent with a query represented as an RGBD goal image o_g . The agent first localizes itself on the graph based on its current observation o_c , and plans a path to reach o_g . From the planned path, the agent picks a subgoal observation o_{sg} and moves towards it using its controller. The agent then relocalizes itself on the graph using its latest observation, then updates the graph. These processes are repeated until the robot reaches o_g .

A. Controller, Reachability, and Waypoint Prediction Model

We train a convolutional neural network $f : \mathcal{I} \times \mathcal{I} \mapsto \{0, 1\} \times SE(2)$ that takes two images and jointly predicts the probability of reachability r from one image to the other, and their relative transformation represented as a waypoint $w = [dx, dy, d\theta]$. For practicality, we only consider w to be valid for reachable image pairs. We train our model by minimizing the binary cross-entropy for reachability, and L_2 loss for the relative waypoint (where heading is encoded as a $[\sin(d\theta), \cos(d\theta)]$ pair). We also calibrate the reachability estimator using Platt scaling [13].

In this work, we use a position-based feedback controller to execute predicted waypoints. Similar to Meng *et al.* [5], we define node-to-node reachability to be controller-dependent. In our case, we assume a simple control strategy based on motion primitives, which imposes simple geometric constraints. Specifically, two nodes should be connected if:

- 1) Visual overlap ratio between the two images, p , is larger than P_{min} , computed based on depth data;
- 2) The ratio of the shortest feasible path length over Euclidean distance between the poses, r_d , is larger than R_{min} , to filter out obstacle-laden paths;
- 3) The target pose must be visible in the initial image, so that our model can visually determine reachability;
- 4) The Euclidean distance to the target must be less than E_{max} , and the relative yaw must be less than Θ_{max} .

During training, we define o_j to be reachable only if it is in front of o_i . Yet, when navigating, the robot can move from o_j to o_i by following the predicted waypoint w in reverse.

B. Graph Building, Planning, and Localization

Instead of using all images in \mathcal{T} , we build the graph G incrementally, as seen in Algorithm 1. We initialize G as a randomly drawn node $o \in \mathcal{T}$. Then, in each iteration, we sample a node $o_{rand} \in \mathcal{T}$, check if it can be merged with or connected to existing graph vertices, and if so, remove it from \mathcal{T} . Concretely, let the geodesic distance of a predicted waypoint be $d(w) = \|\log T(w)\|_F$, where $T(\cdot)$ converts a waypoint into its transformation matrix representation in $SE(2)$ [14]. The node o_{rand} is mergeable to an existing graph vertex if $d(w) < D_{merge}$ in either direction. To determine node-to-node connectivity, we check if reachability $r > \epsilon$, the Euclidean distance $e = \|[dx, dy]\|_2 < \delta_e$, and the

Algorithm 1 Graph Building

Input: trajectory data \mathcal{T} , reachability score threshold ϵ , Euclidean distance threshold δ_e , yaw threshold δ_θ , and merging threshold D_{merge}
Output: graph $G = (V, E)$
Initialize: $V = \{o \in \mathcal{T}\}$, $E = \emptyset$
while there are still connectable nodes in \mathcal{T} **do**
 Sample random node $o_{rand} \in \mathcal{T}$
 for all $o_j \in V$ **do**
 $(r_f, w_f) \leftarrow f(o_{rand}, o_j)$
 $(r_b, w_b) \leftarrow f(o_j, o_{rand})$
 if $r_f > r_b$ **and** (r_f, w_f) satisfy connectivity test **then**
 Connect o_{rand} to o_j with $d(w_f)$ as the weight
 end if
 if $r_b > r_f$ **and** (r_b, w_b) satisfy connectivity test **then**
 Connect o_j to o_{rand} with $d(w_b)$ as the weight
 end if
 end for
 if o_{rand} is connectable or mergeable **then**
 remove o_{rand} from \mathcal{T}
 end if
end while
Return: G

relative yaw angle $d\theta < \delta_\theta$. If o_{rand} is deemed connectable to graph nodes, each new edge is assigned $d(w)$ as weight.

Once the graph is built, we use Dijkstra's algorithm [15] to find a path to a given goal vertex, and select the first node in the path as subgoal o_{sg} . To localize the agent's current observation o_c , we use our model to compare pairwise geodesic distances between o_c and all nodes in the graph, to identify the closest vertex. We also require the reachability score between o_c and the closest node to be larger than ϵ_ℓ , and the geodesic distance between them to be smaller than δ_ℓ . To save computational cost, we first attempt to localize locally by considering only directly adjacent vertices from nodes within the last planned path, and then reverting to global localization among all graph nodes if it fails.

C. Edge Traversal and Graph Updates

Once we identify o_{sg} , we predict its relative waypoint from o_c , and use the controller to move towards it. Then, we update o_c to be the latest observation, and check if edge traversal was successful: either if o_c localizes to o_{sg} , or, if our model's predicted waypoint distance to o_{sg} is below D_{min} .

Since we built the graph using a predictive model, it is important to address the possibility of spurious edges. We propose two types of continuous graph refinements, towards lifelong navigation. Firstly, as seen in Fig. 3, when traversing an edge, we can update both its connectivity and weight based on the success of traversal, z , modeled as a Bernoulli random variable. Letting the prior $p(x)$ be the predicted reachability score, and given an empirically-tuned likelihood parameter $p(z|x)$ of the edge's existence, we can compute the posterior $p(x|z)$ using Bayesian update. When the agent fails to reach a subgoal, it decreases the

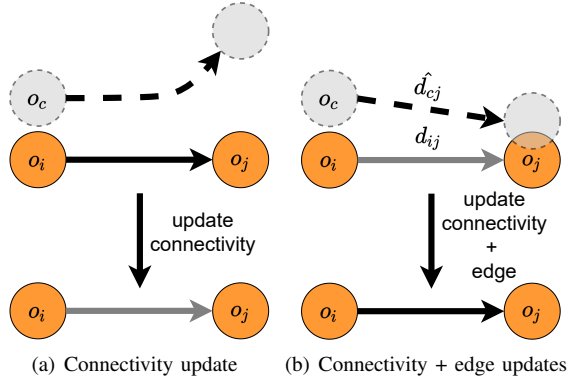


Fig. 3. Illustration of graph update as the agent moves from o_i to o_j . If the agent diverges from the target, we reduce connectivity between o_i and o_j probabilistically, then prune the edge if the updated reachability score falls below R_p . Otherwise, we update both the connectivity and the edge weight based on the predicted geodesic distance \hat{d}_{cj} .

edge’s reachability score, and further prunes the edge if reachability falls below R_p . As for edge weights, we model each prior d_{ij} as a Gaussian around its geodesic distance $d(w)$, and with a common variance derived empirically from our model’s distance predictions for a validation dataset. Only upon success in traversing an edge from our current image o_c to o_j , we treat the predicted geodesic distance \hat{d}_{cj} as measurement, and compute the weight posterior akin to a Kalman filter update step [16].

As a second type of lifelong graph update, we add *new* nodes to the graph either when they are novel or when we cannot find a path to the goal. Concretely, an observation o_c is considered novel when we fail to localize it on the graph. When connecting a novel node to existing vertices, we loosen the graph building criteria, especially to accommodate adding locations around sharp turns. On the other hand, when we are unable to find a path during navigation, we iteratively sample from remaining trajectory nodes \mathcal{T} and *tentatively* add them to the graph G , until a path is found. We then keep only new nodes in G that are along the found path, while returning other tentative nodes back into \mathcal{T} .

D. Real-World Finetuning

A key feature of our method is the ability to finetune our model in the target domain, by using the same trajectories collected to build the graph. Although other methods like ViNG can also finetune on target-domain trajectories, our model can improve performance efficiently using a small finetuning dataset, as it has already been well-trained to navigate within a diverse range of simulated environments.

As an added requirement for real-world finetuning, the collected trajectories must have associated pose odometry to substitute for ground-truth pose data. Thankfully, odometry is readily available from commodity robot sensors such as inertial measurement units or wheel encoders.

For real-world trajectories, we determine node-to-node reachability using the same goal-visibility and maximum-waypoint criteria as when labeling data in simulation. Additionally, since image-to-image visual overlap and shortest

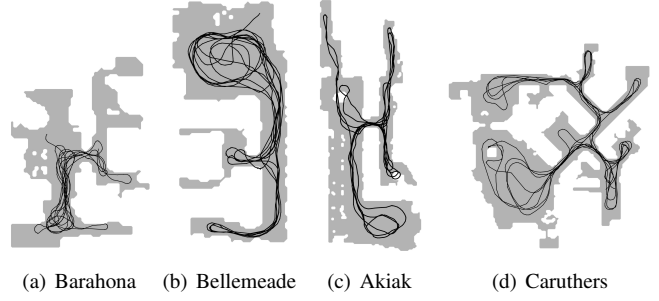


Fig. 4. Top-down view of the agent’s trajectory in each simulated test environment during trajectory collection phase (not to scale).

feasible path length are not readily obtainable in real-world deployment, as a proxy criterion we take an observation pair $(o_i, o_j) \in \mathcal{T}$ where $j > i$ and check if they are separated by at most H time steps during trajectory collection. Using odometry as supervisory signal for predicting waypoints can be noisy. However, since reachable waypoints must be temporally close, the long-term pose drift should be minimal.

IV. EXPERIMENTAL RESULTS

A. Setup

We use Gibson [17] to quantify navigation performance in simulation, and 10 of the interactive environments from iGibson [18] to generate training datasets. We collect 288,000 data points to train our model, and 500,000 data points for SPTM and ViNG, where the width and height of each RGBD observation are 96×72 . We use the LoCoBot [19] in both simulated and real-world experiments, and we teleoperate it in each test map to collect trajectories for building the graph.

B. Evaluation Settings

We evaluate navigation performance to reflect real-world usage: the agent should be able to navigate between any image pairs from the graph, and should not just repeat trajectories based on how the images were collected. We pick several goal images from different locations that covers major locations in each map, and generate random test episodes. In simulation, we consider navigation as successful if the position and yaw errors from the goal pose are less than 0.72m and 0.4 radians. We consider an episode to be a failure if the agent collides for more than 20 times, and if it requires more than K simulation steps to reach the goal. For the real-world experiments, an episode is deemed successful if it finishes within 10 minutes, does not collide with the environment, and we verify that its final observation has sufficient visual overlap with the goal image.

During operations, if the agent is unable to localize itself or find a path, we rotate it in-place and take new observations until it recovers. In addition, to ensure fair comparison with other methods, instead of training an inverse dynamics model for SPTM, we let it to use the same controller as ours and ViNG by coupling it with a pose estimator.

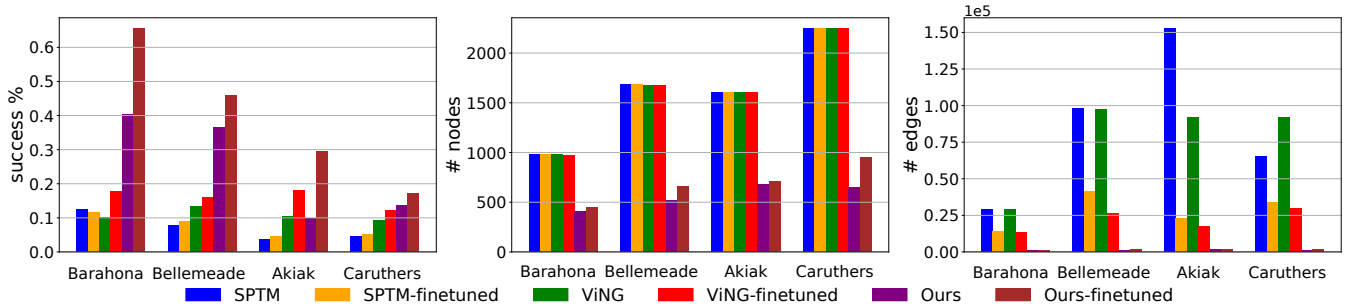


Fig. 5. Comparison of navigation success rates and graph sizes among topological visual navigation methods in various test environments. For visual results of our experiments, including real-world deployment videos, see our project page: <https://montrealrobotics.ca/ltvn/>.

C. Navigation Performance in Simulation

In this section, we compare the navigation performance of our method against SPTM and ViNG in the simulated environments. In this set of experiments, note that *we do not perform graph updates with our method*, which is evaluated separately in Section IV-D.

We evaluate on four test environments that are different from the model’s training maps: Barahona (57m²), Bellemeade (70m²), Akiak (124m²), and Caruthers (129m²). For the graph building phase, we teleoperate the robot to explore roughly 3–4 loops around each map, resulting in 985, 1,685, 1,609, 2,243 images for Barahona, Bellemeade, Akiak, and Caruthers, respectively. Fig. 4 visualizes the top-down view of each test environment with its corresponding trajectory. We pick 10 goal images spanning major locations in each map and generate 500 random test episodes. Given diverse map sizes, we set $K = 1,000$ steps for Barahona and Bellemeade, and $K = 2,000$ steps for Akiak and Caruthers.

As seen in Fig. 5, our method consistently yields higher navigation success rates in all test environments when the model is finetuned. Additionally, our graphs have significantly fewer number of nodes and edges, which helps to keep planning costs practical when scaling to large environments. Therefore, compared to the baselines that use entire trajectory datasets to build graphs, our sampling-based graph building method produces demonstrably superior performance and efficiency.

Fig. 6 qualitatively compares sample graphs built using different methods. We see that our graph has the fewest number of vertices, yet still maintains proper map coverage. Visually, our graph also has few false-positive edges through walls, and we shall later demonstrate how our graph updates can prune these in Section IV-D.

In comparison, the SPTM graph also has few false-positive edges. However, because edges are unweighted in SPTM, anecdotally its agent often chose spurious edges during navigation. With ViNG, since it uses the discretized temporal distance to weigh edges, its graph has many false positive edges with large weights. This becomes problematic when the goal is far away from the robot, as the planned path will likely include some spurious edges. This also leads to an unwanted behavior where the agent always outputs a path no matter how unlikely it is to reach the goal.

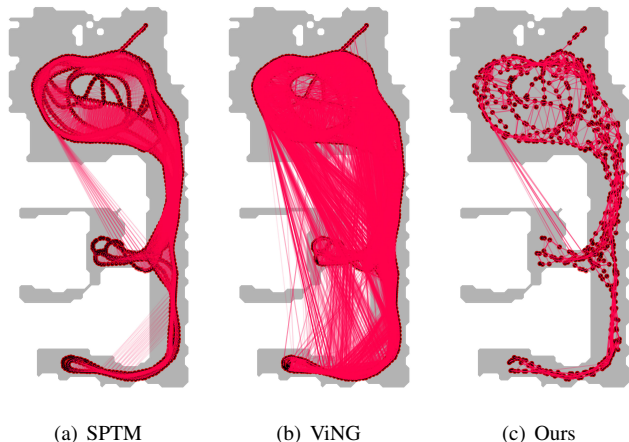


Fig. 6. Graphs built after model finetuning in Bellemeade.

D. Lifelong Improvement

We now evaluate the proposed graph update method to see how navigation performance is affected as the agent performs more queries. We start these experiments using graphs built with our finetuned models. We then ask the agent to execute randomly sampled navigation tasks while performing continuous graph updates. After every 100 queries, we re-evaluate the navigation performance on the same static set of test episodes used in Section IV-C.

As seen in Fig. 7, the success rate generally improves as we perform more queries, with notable gains initially, while the number of nodes and edges in the graph do not substantially grow. We also see an initial *decrease* in the number of edges, suggesting that our graph updates successfully pruned spurious edges causing initial navigation failures, then later added useful new nodes for better navigation. Qualitatively, we can see fewer spurious edges when comparing sample graphs before and after updates in Fig. 8.

We observe that sometimes the success rate decreased after a batch of graph updates. This is likely caused by spurious edges when adding new graph nodes near each 100th query, before we re-evaluate navigation performance. Nevertheless, such spurious edges are pruned in later updates, thus leading to increasing performance trends during lifelong navigation.

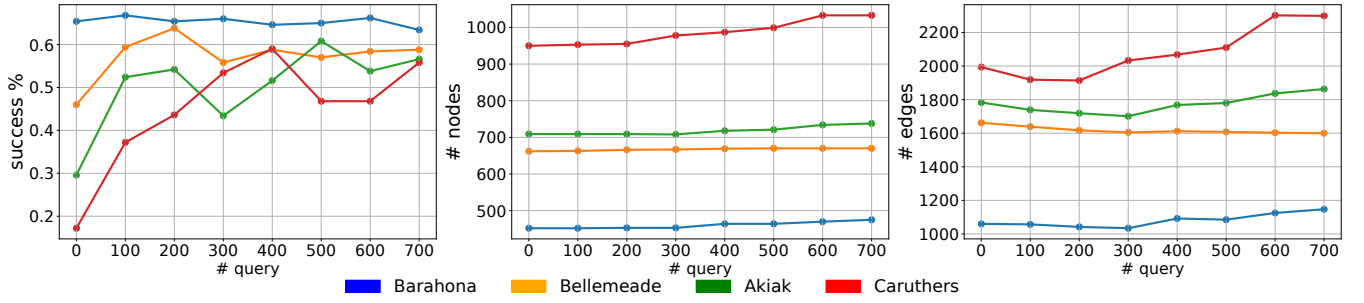


Fig. 7. Changes in success rate, number of nodes, and number of edges as the agent performs more queries and update its graph in each test environment.

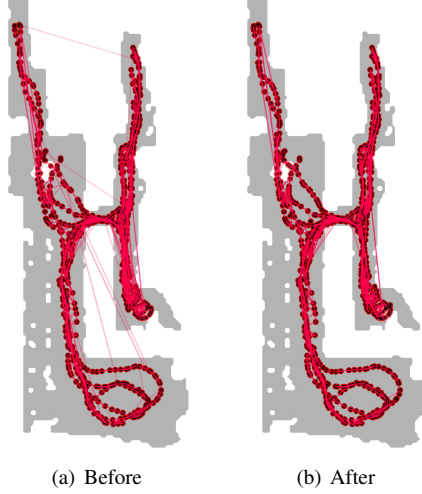


Fig. 8. Graphs before and after 700 query updates in Akiak depict a notable reduction in spurious edges across walls.

E. Real-World Experiments

We evaluate the performance of our method in two real-world environments: a studio apartment and a medium-sized university laboratory. After teleoperating the robot in 3 – 4 loops around each space to collect trajectory data, we pick 5 goal images, and generate 20 test episodes. We use the iLQR [20] implementation from the PyRobot [21] library for our controller. In Table I, we report navigation success rates before and after we perform graph updates with 30 queries.

These experiments confirm that our model performs well without needing large amounts of real-world data, especially when combined with our proposed graph update method. Our graph update method enhances the navigation performance with more than $3\times$ increase in success rate in both envi-

TABLE I
NAVIGATION SUCCESS RATE BEFORE AND AFTER GRAPH UPDATES IN REAL-WORLD ENVIRONMENTS.

	Before	After
Apartment	4/20	13/20
University Laboratory	4/20	14/20

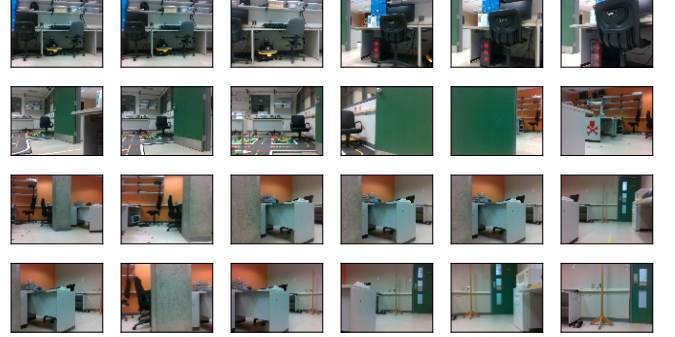


Fig. 9. Sequence of images seen by the robot in the lab environment when navigating from top-left to the bottom-right image.

ronments. Fig. 9 depicts a successful navigation task across multiple twists and turns within the lab environment.

V. CONCLUSIONS

We proposed a new image-based topological graph construction method that applies a sampling-based map building approach. The resulting topological visual navigation system not only produces sparser graphs compared to baseline methods, it also leads to higher navigation performance. This system combines classical graph-based navigation with neural-based learning to enable the agent to update the graph continuously during navigation. Our experiments show that these graph updates add useful new nodes and remove spurious edges, thus increasing performance throughout lifelong navigation. We also demonstrated a training regime using purely simulated data, combined with optional finetuning using small amounts of data from a target domain. Our real-world experiments showed that such deployment and finetuning resulted in significant gains in navigation performance.

While our graph update methods demonstrated promising results, its efficacy in only adding useful graph information can be further improved, especially when sampling new nodes to add when path planning fails. In addition, our model finetuning method relies on expertly piloted trajectories with added odometry information, while it could be more practical to finetune on unordered set of images. Furthermore, in this work we consider the world to be static; extending to non-stationary environments remains a fruitful challenge.

ACKNOWLEDGMENT

The authors would like to thank Mitacs and Element AI (a ServiceNow company) for the support in this project. R. W. thanks IVADO for the support, as well as K. M. Jatavallabhula for useful discussions and feedbacks. L.P. is supported by the Canada CIFAR AI Chairs Program. The work was also supported by the National Science and Engineering Research Council of Canada under the Discovery Grant Program.

REFERENCES

- [1] J. Leonard and H. Durrant-Whyte, "Simultaneous map building and localization for an autonomous mobile robot," in *Proceedings IROS '91: IEEE/RSJ International Workshop on Intelligent Robots and Systems '91*, 1991, pp. 1442–1447 vol.3.
- [2] B. J. Kuipers and T. S. Levitt, "Navigation and mapping in large scale space," *AI Magazine*, vol. 9, no. 2, p. 25, Jun. 1988. [Online]. Available: <https://ojs.aaai.org/index.php/aimagazine/article/view/674>
- [3] Y. Zhu, R. Mottaghi, E. Kolve, J. J. Lim, A. Gupta, L. Fei-Fei, and A. Farhadi, "Target-driven visual navigation in indoor scenes using deep reinforcement learning," in *2017 IEEE international conference on robotics and automation (ICRA)*. IEEE, 2017, pp. 3357–3364.
- [4] N. Savinov, A. Dosovitskiy, and V. Koltun, "Semi-parametric topological memory for navigation," in *International Conference on Learning Representations*, 2018. [Online]. Available: <https://openreview.net/forum?id=SygwwGbRW>
- [5] X. Meng, N. Ratliff, Y. Xiang, and D. Fox, "Scaling local control to large-scale topological navigation," in *2020 IEEE International Conference on Robotics and Automation (ICRA)*. IEEE, 2020, pp. 672–678.
- [6] D. Shah, B. Eysenbach, G. Kahn, N. Rhinehart, and S. Levine, "Ving: Learning open-world navigation with visual goals," *arXiv preprint arXiv:2012.09812*, 2020.
- [7] L. Kavraki, P. Svestka, J.-C. Latombe, and M. Overmars, "Probabilistic roadmaps for path planning in high-dimensional configuration spaces," *IEEE Transactions on Robotics and Automation*, vol. 12, no. 4, pp. 566–580, 1996.
- [8] S. M. LaValle *et al.*, "Rapidly-exploring random trees: A new tool for path planning," 1998.
- [9] Y. Wu, Y. Wu, A. Tamar, S. Russell, G. Gkioxari, and Y. Tian, "Bayesian relational memory for semantic visual navigation," in *Proceedings of the IEEE International Conference on Computer Vision*, 2019, pp. 2769–2779.
- [10] S. Nasiriany, V. Pong, S. Lin, and S. Levine, "Planning with goal-conditioned policies," in *Advances in Neural Information Processing Systems*, H. Wallach, H. Larochelle, A. Beygelzimer, F. d'Alché-Buc, E. Fox, and R. Garnett, Eds., vol. 32. Curran Associates, Inc., 2019.
- [11] B. Eysenbach, R. R. Salakhutdinov, and S. Levine, "Search on the replay buffer: Bridging planning and reinforcement learning," in *Advances in Neural Information Processing Systems*, H. Wallach, H. Larochelle, A. Beygelzimer, F. d'Alché-Buc, E. Fox, and R. Garnett, Eds., vol. 32. Curran Associates, Inc., 2019.
- [12] S. Emmons, A. Jain, M. Laskin, T. Kurutach, P. Abbeel, and D. Pathak, "Sparse graphical memory for robust planning," in *Advances in Neural Information Processing Systems*, H. Larochelle, M. Ranzato, R. Hadsell, M. F. Balcan, and H. Lin, Eds., vol. 33. Curran Associates, Inc., 2020, pp. 5251–5262.
- [13] C. Guo, G. Pleiss, Y. Sun, and K. Q. Weinberger, "On calibration of modern neural networks," in *Proceedings of the 34th International Conference on Machine Learning*, ser. Proceedings of Machine Learning Research, D. Precup and Y. W. Teh, Eds., vol. 70. PMLR, 06–11 Aug 2017, pp. 1321–1330. [Online]. Available: <http://proceedings.mlr.press/v70/guo17a.html>
- [14] T. D. Barfoot, *State Estimation for Robotics*, 1st ed. USA: Cambridge University Press, 2017.
- [15] E. W. Dijkstra, "A note on two problems in connexion with graphs," *Numer. Math.*, vol. 1, no. 1, p. 269–271, Dec. 1959. [Online]. Available: <https://doi.org/10.1007/BF01386390>
- [16] R. E. Kalman, "A New Approach to Linear Filtering and Prediction Problems," *Journal of Basic Engineering*, vol. 82, no. 1, pp. 35–45, 03 1960. [Online]. Available: <https://doi.org/10.1115/1.3662552>
- [17] F. Xia, A. R. Zamir, Z.-Y. He, A. Sax, J. Malik, and S. Savarese, "Gibson env: real-world perception for embodied agents," in *Computer Vision and Pattern Recognition (CVPR), 2018 IEEE Conference on*. IEEE, 2018.
- [18] B. Shen, F. Xia, C. Li, R. Martín-Martín, L. Fan, G. Wang, S. Buch, C. D'Arpino, S. Srivastava, L. P. Tchaptzi, K. Vainio, L. Fei-Fei, and S. Savarese, "igibson, a simulation environment for interactive tasks in large realistic scenes," *arXiv preprint*, 2020.
- [19] "Locobot - an open source low cost robot," <http://www.locobot.org/>, accessed: 2021-09-14.
- [20] W. Li and E. Todorov, "Iterative linear quadratic regulator design for nonlinear biological movement systems," in *ICINCO 2004, Proceedings of the First International Conference on Informatics in Control, Automation and Robotics, Setúbal, Portugal, August 25-28, 2004*, H. Araújo, A. Vieira, J. Braz, B. Encarnação, and M. Carvalho, Eds. INSTICC Press, 2004, pp. 222–229.
- [21] A. Murali, T. Chen, K. V. Alwala, D. Gandhi, L. Pinto, S. Gupta, and A. Gupta, "Pyrobot: An open-source robotics framework for research and benchmarking," *arXiv preprint arXiv:1906.08236*, 2019.